Protein Science (2000), *9*:1274–1281. Cambridge University Press. Printed in the USA.

Topography of a 2.0 Å structure of α_1-antitrypsin reveals targets for rational drug design to prevent conformational disease

PETER R. ELLIOTT, XUE Y. PEI, TIMOTHY R. DAFFORN, AND DAVID A. LOMAS

Respiratory Medicine Unit, Department of Medicine and Department of Haematology, University of Cambridge, The Wellcome Trust Centre for Molecular Mechanisms in Disease, Cambridge Institute for Medical Research, Wellcome Trust/MRC Building, Hills Road, Cambridge CB2 2XY, United Kingdom

(RECEIVED February 8, 2000; FINAL REVISION April 17, 2000; ACCEPTED April 28, 2000)

Abstract

Members of the serpin family of serine proteinase inhibitors play important roles in the inflammatory, coagulation, fibrinolytic, and complement cascades. An inherent part of their function is the ability to undergo a structural rearrangement, the stressed (S) to relaxed (R) transition, in which an extra strand is inserted into the central A β-sheet. In order for this transition to take place, the A sheet has to be unusually flexible. Malfunctions in this flexibility can lead to aberrant protein linkage, serpin inactivation, and diseases as diverse as cirrhosis, thrombosis, angioedema, emphysema, and dementia. The development of agents that control this conformational rearrangement requires a high resolution structure of an active serpin. We present here the topology of the archetypal serpin α_1-antitrypsin to 2 Å resolution. This structure allows us to define five cavities that are potential targets for rational drug design to develop agents that will prevent conformational transitions and ameliorate the associated disease.

Keywords: α_1-antichymotrypsin; α_1-antitrypsin; antithrombin; molecular surface; PAI-1; polymerization; SURFNET; topography

The serpins are a family of serine proteinase inhibitors that have been identified in a wide variety of viruses, plants, and higher organisms (Potempa et al., 1994). To date, more than 70 different serpins have been reported and more are being identified. They act to control proteinases involved in the inflammatory, coagulation, fibrinolytic, and complement cascades. Serpins also function as hormone carriers (thyroxine and cortisol binding globulin), as peptide donors in the control of blood pressure (angiotensinogen), and as chaperones (HSP-40) and storage proteins (ovalbumin). Crystal structures have shown the serpins to have remarkable structural homology characterized by a dominant A β-sheet and a mobile reactive center loop that presents a peptide sequence as the substrate for the target proteinase. Following docking the loop is cleaved at the P_1-P_1' bond and the enzyme is locked into an irreversible SDS-stable complex (Lawrence, 1997).

The flexibility of the reactive loop has been demonstrated by a remarkable series of crystal structures. The early serpin structures showed the P_1-P_1' residues separated by 70 Å following reactive loop cleavage (Fig. 1A) with the amino-terminal region of the reactive center loop incorporated as strand 4 into the A β-sheet (Loebermann et al., 1984; Engh et al., 1989; Delarue et al., 1990; Baumann et al., 1991, 1992; Mourey et al., 1993). This cleaved or relaxed (R) conformation of the reactive loop was clearly incompatible with function as a proteinase inhibitor and the crystal structures of intact ovalbumin (Stein et al., 1990), α_1-antichymotrypsin (Wei et al., 1994), antithrombin (Carrell et al., 1994; Schreuder et al., 1994), and more recently PAI-1 (Sharp et al., 1999), PAI-2 (Harrop et al., 1998), and serpin 1K from *Manduca sexta* (Li et al., 1999) have demonstrated that the intact P_1-P_1' bond of the reactive loop is at the apex of the protein. The reactive center loop in these intact or stressed (S) proteins is still not in an ideal configuration to dock with the substrate binding pocket of a target proteinase. As such, they must undergo a conformational re-arrangement upon binding with the enzyme or, in the case of antithrombin, following activation with heparin (Jin et al., 1997). Only in the structures of stabilized (Elliott et al., 1996; Ryu et al., 1996) and wild-type (Elliott et al., 1998) α_1-antitrypsin is the loop held in a conformation that is ideal for docking with the cognate proteinase, in this case neutrophil elastase.

The flexibility of the reactive loop and A β-sheet is required for a serpin to function as an inhibitor but also permits the acceptance of inappropriate peptides. The acceptance of an exogenous reactive loop peptide from another serpin molecule results in a dimer that can then extend to form chains of loop-sheet polymers (Elliott et al., 1996). This process of polymerization occurs spontaneously in mutants of the serpins to cause deficiency of α_1-antitrypsin,

Reprint requests to: David Lomas, Cambridge Institute for Medical Research, Wellcome Trust/MRC Building, Hills Rd., Cambridge CB2 2XY, United Kingdom; e-mail: dal16@cam.ac.uk.

antithrombin, and C1-inhibitor in association with cirrhosis, thrombosis, and angio-oedema, respectively (Stein & Carrell, 1995). Moreover, tissue deposition of polymers of variants of the neurone specific serpin, neuroserpin, underlies an unusual inclusion body dementia (Davis et al., 1999). In some cases, the intact reactive loop of some serpins can be fully incorporated into their own A β-sheet in vivo to form an inactive latent conformation. This occurs spontaneously under physiological conditions in plasminogen activator inhibitor-1 (Mottonen et al., 1992) but can also occur in α_1-antichymotrypsin in association with chronic obstructive pulmonary disease (Chang & Lomas, 1998).

The propensity for naturally occurring mutants of the serpins to cause disease has led us to propose the development of drugs to modulate the conformational transitions (Elliott et al., 1998). To achieve this a high resolution structure of an active serpin is required and the binding sites on the surface of the serpin must be defined. We present here the highest resolution structure obtained to date of an intact serpin. An investigation into the changes that occur in the surface topography of the serpins during the S to R transition has allowed us to define five sites that may be suitable as targets for rational drug design.

Results and discussion

The 2.0 Å structure of native intact α_1-antitrypsin

The high resolution crystal structure of α_1-antitrypsin is illustrated in Figure 1A with a summary of the crystallographic data shown in Table 1. The fold is almost identical to those of Phe51Leu and wild-type α_1-antitrypsin (Elliott et al., 1996, 1998) with the molecule composed of three β-strands (A–C) and 9 α-helices (A–I) and the reactive center loop held at the apex of the protein. As before, the reactive loop has adopted the characteristic extended β-strand canonical conformation between P_3' and P_8. It is stabilized in this conformation by a salt bridge between P_5 glutamate and arginines 196, 223, and 281 in the body of the molecule and lattice contacts between P_4–P_6 and residues 213Val, 214Thr, and 215Thr of the adjacent protein. The improved electron density allows greater confidence in modeling amino acid side chains as is clearly illustrated for the reactive loop in Figure 1B. This demonstrates that the canonical conformation between P_3 and P_3' is stabilized by a water molecule that is hydrogen bonded to the hydroxyl group of 283Ser and the carbonyl oxygens of P_2 (357Pro) and P_1' (359Ser). Close examination of the hinge region of the loop (P_{13}-P_{16}) showed significant differences from the 2.9 Å structures (Elliott et al., 1996, 1998) with both the backbone and side chains being seen with greater clarity. The position of the P_{16} lysine residue can now be redefined facing the backbone of P_9 (350Ala). The position occupied by this residue in the low resolution structures is now seen to be filled by two well-defined water molecules. The repositioning of the P_{16} side chain combined with remodeling of this area led to an improved backbone trace between residues 342Glu (P_{17}) and 351Met (P_8). This change resulted in repositioning of the solvent exposed side chains of residues 345Thr and 346Glu. The 2 Å structure also allowed more detailed modeling of other main- and side-chain residues of the protein (Fig. 1C).

Changes in serpin topography during the S to R transition

The β-strand conformation of the reactive center loop can readily insert into the A β-sheet of a second molecule to form a dimer that then extends as chains of polymers. This process occurs in most serpins if they are heated or treated with denaturants (Mast et al., 1992; Lomas et al., 1993; Patston et al., 1995) but may also occur spontaneously in association with point mutations that cause disease (Stein & Carrell, 1995). The serpin molecule accepts the loop of a second by expansion of the A β-sheet (as seen in the S to R transition) and may therefore be blocked by agents which prevent this movement. A dataset of structures was constructed using serpins for which data exist for both the S and R states: α_1-antitrypsin, PAI-1, antithrombin, and α_1-antichymotrypsin. This allows comparisons of the changes in topography during the S to R transition between serpins that have different functions. Cavities exceeding 200 Å^3 were investigated as these will accept 13 atoms of any therapeutic agent. Five cavities were identified as shown in Figure 2 and detailed in Table 2.

Table 1. *X-ray data collection and processing*

Space group	C2
Cell dimension (Å)	a = 114.68, b = 39.26, c = 90.27, β = 104.21°
Resolution (Å)	25 − 2.0
Wavelength (Å)[a]	0.87
No. of reflections	156,306
No. of unique reflections	25,057
Rmerge (%)[b] overall	7.9 (50.3)
Completeness (%)	93.7[c]
Redundancy	3.3 (2.2[c])
$\langle I/\sigma(I)\rangle$[c]	5.9 (1.5[c])
B_{wilson} (Å^2)[d]	29.4
Resolution (Å) (CNS)	25 − 2.0
R-factor (%)[e]	23.1
R_{free} (%)[f]	26.6
No. of reflections for work set	23,778 (25.0 − 2.0 Å)
No. of reflections for test set	1,272 (25.0 − 2.0 Å)
Weighted root-mean-square deviation from ideality[g]	
Bond lengths (Å)	0.006
Bond angles (deg)	1.306
Total no. of atoms	3,068
No. of water molecules	109

[a]The X-ray diffraction data from a single frozen crystal were collected at Station 9.6, SRS, Daresbury, UK.
[b]$R_{merge} = [\sum\sum|I_j(h) - \langle I(h)\rangle|/(\sum\sum I_j(h)] \times 100$; values in parentheses correspond to highest resolution shell.
[c]For high resolution (2.05 − 2.0 Å).
[d]Calculated with the program TRUNCATE (CCP4, 1994).
[e]$R = \sum||F_{obs}| - k|F_{calc}||/\sum|F_{obs}|$ with k as scaling factor.
[f]Free R-factor calculated with the 4.7% of the data not used during refinement.
[g]With respect to the ideal value.

Cavity 1

Cavity 1 exists as a cleft between the top of s6A and strands 4B and 3C. The cavities in α_1-antitrypsin, α_1-antichymotrypsin, and PAI-1 all increase in volume following the S to R transition, whereas the cavity in antithrombin shrinks. Closer examination of the structural changes shows that in α_1-antitrypsin the change in shape of the cavity is induced almost entirely by rearrangement of the C-terminus of the protein. In particular, the side chain of Thr392

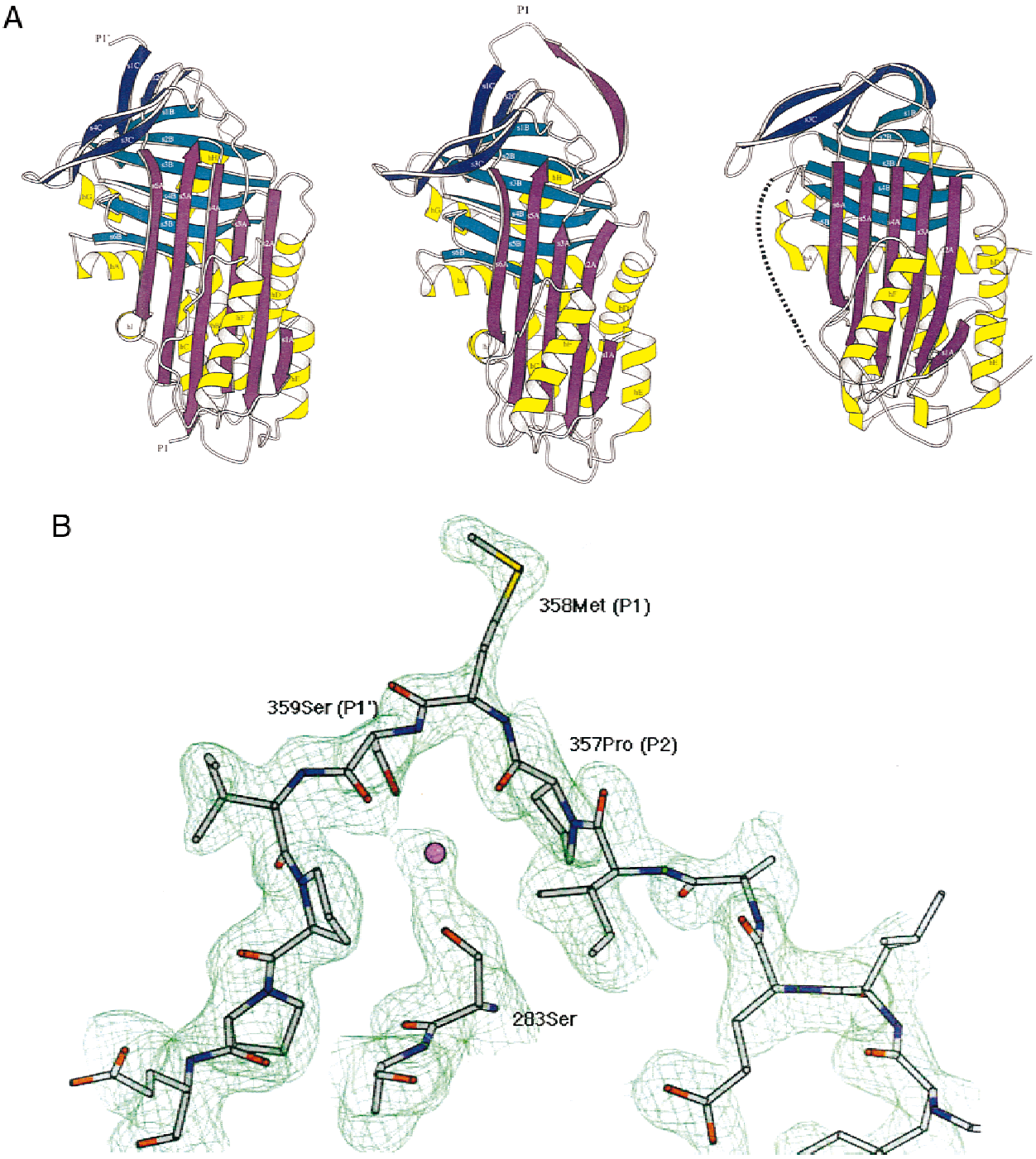

Fig. 1. A: The overall fold of reactive loop cleaved (left) (from (Loebermann et al., 1984)) and native (middle) α_1-antitrypsin demonstrating the insertion of the reactive loop into the A β-sheet as s4A after cleavage at the P_1-P_1' (358Met–359Ser) bond. The intact loop may also be incorporated into the A β-sheet to form a six stranded inactive latent conformation (right). The native conformation represents the stressed (S) form and the reactive loop cleaved and latent species illustrate the relaxed (R) form. Strands A–C and helices A–I are indicated. **B:** The new 2.0 Å resolution structure provides improved density for the reactive loop. The higher resolution shows that the inhibitory canonical structure of the loop is stabilized by a water molecule (purple) that is hydrogen bonded to the hydroxyl group of 283Ser and the carbonyl oxygens of P2 (357Pro) and P_1' (359Ser). Moreover, there were differences in the C-α (**C**, left) and side-chain positioning (**C**, right) when the new structure (black) was compared with the previous 2.9 Å resolution model (grey). (*Figure continues on facing page.*)

Table 2. *A summary of the volumes of the five cavities calculated for four serpins*[a]

Cavity	Protein	Conformation		
		Native	Cleaved	Latent
1	α_1-antitrypsin	58.3	279.5	—
	α_1-antichymotrypsin	196.1	276.5	—
	PAI-1	0	0	492.0
	Antithrombin	**564.7**	**354.3**	412.7
2	α_1-antitrypsin	**285.7**	**91.1**	—
	α_1-antichymotrypsin	0	159.7	—
	PAI-1	**675.8**	**210.9**	**294.4**
	Antithrombin	641.0	678.9	1,316.7
3	α_1-antitrypsin	350.2	420.8	—
	α_1-antichymotrypsin	384.2	378.9	—
	PAI-1	0	245.2	117.2
	Antithrombin	252.9	61.4	74.2
4	α_1-antitrypsin	291.3	140.8	—
	α_1-antichymotrypsin	139.2	344.1	—
	PAI-1	501.7	701.9	652.3
	Antithrombin	480.7	562.7	502.2
5	α_1-antitrypsin	679.4	1,060.9	—
	α_1-antichymotrypsin	859.5	1,283.1	—
	PAI-1	518.6	540.1	774.0
	Antithrombin	482.3	470.0	929.8

[a]The values in bold indicate a decrease in cavity size in excess of 200 Å on transition from the S (native) to R (reactive loop cleaved or latent) conformation in the same serpin.

changes from pointing away from the cavity (in the native form) to pointing directly into the cavity (in the cleaved structure). However, no cavity could be detected in either the native or cleaved form of PAI-1, whereas in the latent form the C-terminus undergoes a change in conformation to move into the space originally filled by the reactive loop linking s1C to s4B. It is the C-terminus that also determines the size and shape of cavity 1 in antithrombin. The largest volume is measured when the C-terminus points away from the cavity (native), and the smallest when the cavity is disrupted by incursion of the C-terminus (cleaved). The size of cavity 1 in α_1-antichymotrypsin is also determined entirely by the positioning of the C-terminus.

Cavity 2

Cavity 2 is the same as that previously identified in a low resolution structure of α_1-antitrypsin (Elliott et al., 1998). This cavity reduces in volume during the S to R transition of α_1-antitrypsin and PAI-1, but increases in antithrombin and α_1-antichymotrypsin. The change from the S to the R state resulted in a 71 and 69% decrease in volume in α_1-antitrypsin and PAI-1, respectively, and is caused solely by the movement of s2A (Fig. 3). This results from s3A being displaced by the insertion of the reactive centre loop into the A sheet as s4A (Fig. 1). Thus, the size of the cavity is defined by the state of the A-sheet and so it seems reasonable to expect that the reverse is true. We can therefore conclude that this cavity would be a good candidate for a drug binding site to control A-sheet opening and conformational disease in α_1-antitrypsin and PAI-1. Closer examination of the cavity using the higher resolution data from the new α_1-antitrypsin structure gives us a more detailed view of the residues involved in forming its boundaries. Figure 4 shows that the pocket is bounded by mainly hydrophilic residues: Ser56, Asn104, Thr114, His139, and Asn186 along with the backbone atoms of Tyr187. The new high resolution structure also shows six water molecules within the cavity. One water molecule forms a hydrogen bond with the main-chain oxygen of Ser56 and two others are hydrogen bonded to each other.

Cavity 3

Cavity 3 is bordered by s6A and by hA and again demonstrates different behaviors between serpins. Both α_1-antitrypsin and PAI-1 show increases in cavity size during the S to R transition, whereas in antithrombin, the cavity collapses. A closer examination of the structures surrounding cavity 3 shows that it is formed by a combination of structural elements. One end of this elongated cavity is made up of the surfaces of hA, s6B, and the C-terminus. The

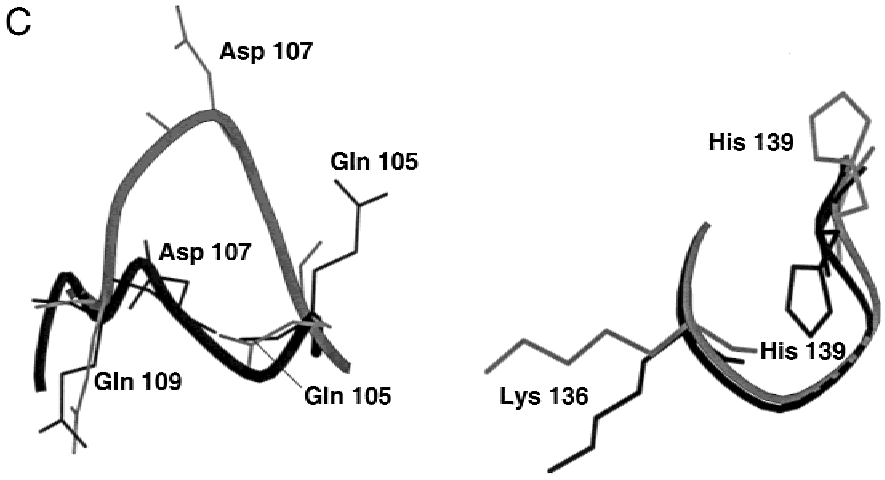

Fig. 1. *Continued.*

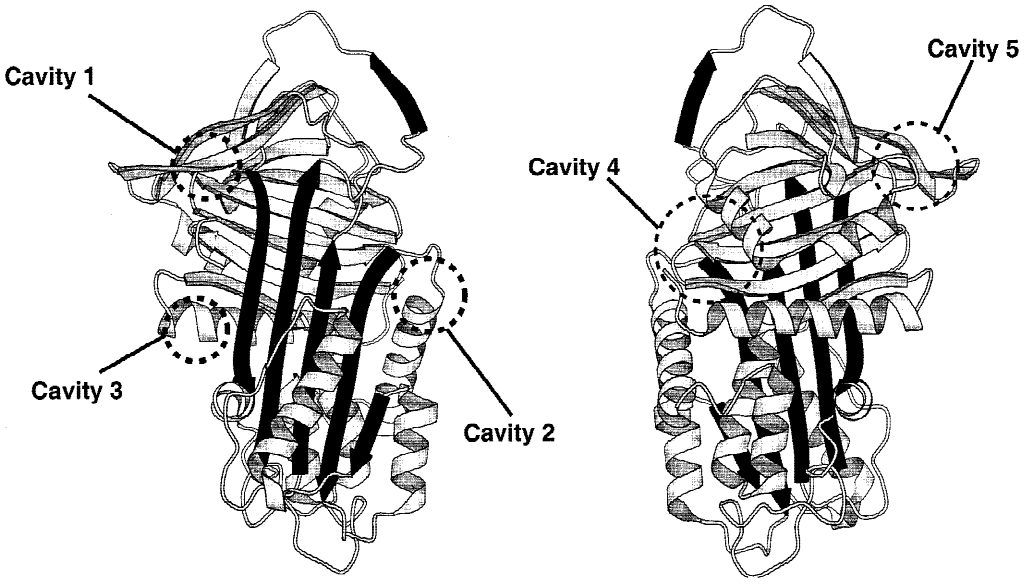

Fig. 2. Surface cavities exceeding 200 Å^3 in volume that are common among the serpins. Left, front view in standard orientation; right, back view.

cavity then stretches across the base of strands 6A and 5A and is terminated by the loop connecting hF and s3A. Comparisons of the shape of the cavity in the native and cleaved form of α_1-antitrypsin show that the increase in volume upon cleavage occurs due to a rearrangement of the hF-s3A loop caused by the introduction of the reactive loop into the A sheet following cleavage. The equivalent cavity in antithrombin is quite different, being more spherical than elongated, as it does not extend over the A sheet as far as in α_1-antitrypsin. The cavity becomes smaller during the S to R transition as one end is filled by movement of the C-terminal end of hA while the other is closed by rearrangements of the side chains of Glu333 and Gln334 on the end of s6A.

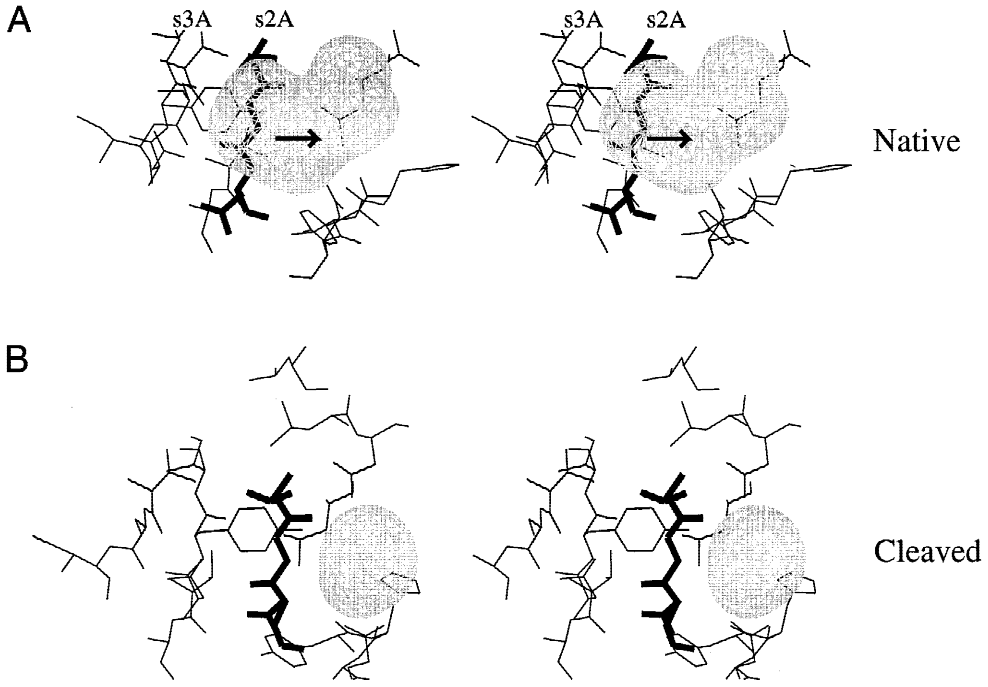

Fig. 3. Stereo diagram showing a comparison of the shape and size of the cavity found within (**A**) native and (**B**) cleaved α_1-antitrypsin. The arrow indicates the direction of movement of s2A (bold) that occurs as a result of the incorporation of the reactive loop into the A β-sheet. This S to R transition is central to the function of the serpins as proteinase inhibitors but the reactive loop peptides of other molecules can also be incorporated into the A β-sheet to form chains of polymers that are associated with disease.

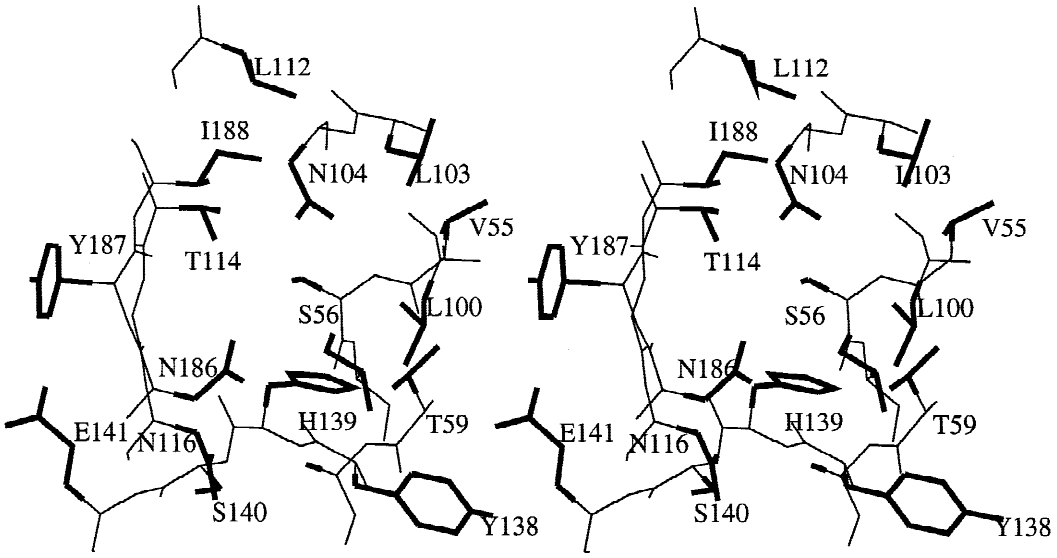

Fig. 4. Stereo diagram of the residues surrounding cavity 2 in the high resolution structure of α_1-antitrypsin. Side chains are depicted in thick lines and backbone in thin lines.

Cavity 4

Cavity 4 is on the face of strands 4B and 5B between hA and hH. Calculation of the dimensions of cavity 4 shows that in all but α_1-antitrypsin this cavity increases in volume as the protein undergoes the S to R transition. Closer inspection shows that one of the bounding areas of cavity 4 is made up by the N-terminal region of serpins. Unfortunately, in most structures this region is ill-defined making any conclusions about the volume changes of cavity 4 unreliable.

Cavity 5

Cavity 5 is sited in a groove formed by the loop between s3C and s4C and helix G. Indeed, it is this groove in which the peptide linking s4A and s1C sits when a serpin adopts the latent conformation. Analysis of the results of the cavity search show that in α_1-antitrypsin and α_1-antichymotrypsin there is a large increase in the volume of this cavity upon cleavage of the reactive loop. This is due entirely to the rearrangement of the s3C/s4C loop as a result of an overall shift in this region caused by the freeing of the C-terminal end of s1C by the cleavage of the P1-P1′ peptide bond. The same behavior does not occur in PAI-1. The cavity in PAI-1 only increases in volume in the latent form of the R state with very little change being seen in the cleaved form. The data from antithrombin for this cavity are similar to PAI-1, with little change in volume seen between the native and cleaved state but a large increase observed upon transition to the latent state. However, in the case of antithrombin, the cavity in the latent state is much larger than that seen for PAI-1. This difference results from the antithrombin cavity expanding to include the cleft left by removal of s1C to form the latent conformation.

Analysis of recombinant and naturally occurring mutants that line cavity 2

Our analysis has demonstrated that cavity 2 is the most suitable for rational drug design to control the conformational transitions of α_1-antitrypsin and PAI-1. If it is indeed true that the area surrounding the cavity is inherently linked to, and important in, the S to R transition then mutations in this area should have significant effects on protein function. The extensive study of a range of human serpins has led to the establishment of a large database of mutations associated with disease (Stein & Carrell, 1995). Comparing the residues highlighted in Figure 4 with this database showed that mutations of residues 55, 56, 59, 112, 114, and 138 have significant effects on protein function. More specifically, Val55Pro causes conformational transitions and plasma deficiency of α_1-antichymotrypsin (Gooptu et al., 2000), Ser56Arg causes polymerization of neuroserpin and an early onset inclusion body dementia (Davis et al., 1999), Thr59Ala increases stability of α_1-antitrypsin (Lee et al., 1996), Ile112Leu and Thr114Ser increase stability in recombinant PAI-1 (Berkenpas et al., 1995), and Tyr138Cys causes antithrombin deficiency and thrombosis (Choudhury et al., 1993). There are also effects on the noninhibitory serpins: Ile100Asn creates a new glycosylation site in thyroxine binding globulin that reduces stability and thyroxine binding affinity (Mori et al., 1989) and Thr114Met in angiotensinogen has been associated with hypertension (Jeunemaitre et al., 1992). Two of these cavity residues, Ser56 and Asn186, are conserved in over 75% of serpin sequences (Whistock, 1996). Further support for the significance of this cavity comes from mutational studies of PAI-1, which have been used to define the binding site of vitronectin (Sui & Wiman, 1998) and a small molecule inhibitor (Björquist et al., 1998). Both ligands are predicted to effect the state of the A-sheet in PAI-1. In both cases, the binding sites were localized to the region along the edge of s2A, hD, and hE. This area overlays the entrance of cavity 2.

The chemical properties of cavity 2 were then assessed in the other serpins used in this study. This allowed predictions of the chemical determinants required by a putative drug to allow both good binding and selectivity. Examination of cavity 2 in α_1-antitrypsin showed it to be lined by hydrophobic and uncharged hydrophilic residues. These hydrophilic residues provide a number of hydrogen bonding opportunities to a binding ligand. Analysis of cavity 2 in antithrombin and PAI-1 showed them to be lined by

similar residues. However, of greater importance is the question of serpin selectivity in drug design. Comparisons of the size of the entrance of cavity 2 in antithrombin, α_1-antitrypsin, and PAI-1 showed some significant differences. α_1-Antitrypsin has a large entrance to cavity 2, bordered by the loops between helix D and s2C, helix E and s1C and the edge of s2C. In contrast, both antithrombin and PAI-1 have entrances that are narrowed by the incursions of bulky residues (Tyr79 and Met83 in PAI-1 and Tyr131 in antithrombin). Thus, specificity for α_1-antitrypsin could be conferred on a drug by ensuring that it was large enough to be excluded from the cavities in PAI-1 and antithrombin while still fitting into cavity 2 of α_1-antitrypsin.

Taken together, these data provide strong support for our conclusion that cavity 2 represents the best candidate for therapies to prevent conformational disease in α_1-antitrypsin. Our high resolution structure of α_1-antitrypsin demonstrates the dimensions of this cavity thereby providing a firm foundation for rational drug design.

Materials and methods

Expression and crystallization of recombinant α_1-antitrypsin

Recombinant wild-type α_1-antitrypsin was expressed, purified to homogeneity, and characterized as detailed previously (Elliott et al., 1998). The purified protein was 70% active as an inhibitor of bovine α-chymotrypsin and migrated as a characteristic doublet on SDS-PAGE with the proportion of protein in each band varying between batches. The heterogeneity was caused by the cleavage of 7 or 11 N-terminal amino acids but this did not affect crystallization. Wild-type α_1-antitrypsin crystals were grown in 6 μL hanging drops equilibrated against 24% (w/v) PEG 4000, 0.2 M NaOAc, 0.1 M Tris·HCl pH 6.0, 2 mM $FeSO_4 \cdot 7H_2O$ at 18 °C over four weeks. The crystal was momentarily immersed in mother liquor containing 20% (v/v) methylpentane diol cyroprotectant and rapidly frozen to 100 K in the cryostream of an Oxford Cryosystems cryocooler. Diffraction data were collected from a single frozen crystal on station 9.6 at the Daresbury Synchrotron (Warrington, U.K.) using an ADSC Quantum4 CCD detector and monochromatic X-rays of 0.87 Å wavelength. The crystal diffracted to 2.0 Å resolution.

Data processing and structure refinement

Data were integrated with MOSFLM (Leslie, 1992) and processed with programs from the CCP4 suite (CCP4, 1994). The initial phases were obtained by molecular replacement with AMORE (Navaza, 1994) using 8 to 4 Å data and our previous 2.9 Å structure of wild-type α_1-antitrypsin (2 psi) as a search molecule (Elliott et al., 1998). This generated a model with an *R*-factor of 30.4% and a correlation coefficient of 0.737. Following rigid body refinement, constant *B*-factor refinement using maximum likelihood refinement and all the data from 25.0 to 2.0 Å, the model had a free *R*-factor of 37.3%. Further rounds of restrained refinement using Protin (Machin et al., 1980), RefMac (Murshudov et al., 1997), and model building with "O" (Jones et al., 1991) brought the free *R*-factor down to 32.9%. To adequately model the bulk solvent contribution, further rounds of refinement were carried out using CNS (Read, 1986; Brünger et al., 1987, 1990, 1997; Brünger, 1992; Rice & Brünger, 1994; Kleywegt & Brünger, 1996; Pannu & Read, 1996; Adams et al., 1997) resulting in significant improvements in the free *R*-factor (Table 1). The figures were prepared with MOLSCRIPT (Kraulis, 1991).

Cavity search techniques

The accessible surface cavities of four serpins in a variety of conformations (native α_1-antitrypsin, cleaved α_1-antitrypsin (Loebermann et al., 1984), native PAI-1 (Sharp et al., 1999), cleaved PAI-1 (Aertgeerts et al., 1995), native antithrombin (Skinner et al., 1997), cleaved antithrombin (Mourey et al., 1993), latent antithrombin (Skinner et al., 1997), native α_1-antichymotrypsin (Wei et al., 1994), and cleaved α_1-antichymotrypsin (Baumann et al., 1991)) were calculated using the appropriate X-ray crystal structures and the program SURFNET (Laskowski, 1995). Solvent was removed from each structure and the coordinates analyzed by SURFNET using a grid separation of 0.8 and a minimum and maximum radii for the gap spheres of 2.0 and 4.0 Å, respectively.

Acknowledgments

We are grateful to Prof. Randy J. Read for his help with the crystallographic analysis. This work was supported by the Wellcome Trust and the British Heart Foundation.

References

Adams PD, Pannu NS, Read RJ, Brünger AT. 1997. Cross-validation maximum likelihood enhances crystallographic simulated annealing refinement. *Proc Natl Acad Sci 94*:5018–5023.

Aertgeerts K, De Bondt HL, De Ranter CJ, Declerck PJ. 1995. Mechanisms contributing to the conformational and functional flexibility of plasminogen activator inhibitor-1. *Nat Struct Biol 2*:891–897.

Baumann U, Bode W, Huber R, Travis J, Potempa J. 1992. Crystal structure of cleaved equine leucocyte elastase inhibitor determined at 1.95 Å resolution. *J Mol Biol 226*:1207–1218.

Baumann U, Huber R, Bode W, Grosse D, Lesjak M, Laurell C-B. 1991. Crystal structure of cleaved human α_1-antichymotrypsin at 2.7 Å resolution and its comparison with other serpins. *J Mol Biol 218*:595–606.

Berkenpas MB, Lawrence DA, Ginsburg D. 1995. Molecular evolution of plasminogen activator inhibitor-1 functional stability. *EMBO J 14*:2969–2977.

Björquist P, Ehnebom J, Inghardt T, Hansson L, Lindberg M, Linschoten M, Strömqvist M, Deinum J. 1998. Identification of the binding site for a low-molecular-weight inhibitor of plasminogen activator inhibitor type 1 by site-directed mutagenesis. *Biochemistry 37*:1227–1234.

Brünger AT. 1992. The free *R* value: A novel statistical quantity for assessing the accuracy of crystal structures. *Nature 355*:472–474.

Brünger AT, Adams PD, Rice LM. 1997. New applications of simulated annealing in X-ray crystallography and solution NMR. *Structure 5*:325–336.

Brünger AT, Krukowski A, Erickson J. 1990. Slow-cooling protocols for crystallographic refinement by simulated annealing. *Acta Crystallogr A46*:585–593.

Brünger AT, Kuriyan J, Karplus M. 1987. Crystallographic *R* factor refinement by molecular dynamics. *Science 235*:458–460.

Carrell RW, Stein PE, Fermi G, Wardell MR. 1994. Biological implications of a 3 Å structure of dimeric antithrombin. *Structure 2*:257–270.

CCP4 (Collaborative Computational Project Number 4). 1994. Programs for protein crystallography. *Acta Crystallogr D50*:760–763.

Chang W-SW, Lomas DA. 1998. Latent α_1-antichymotrypsin: A molecular explanation for the inactivation of α_1-antichymotrypsin in chronic bronchitis and emphysema. *J Biol Chem 273*:3695–3701.

Choudhury V, Olds RJ, Lane DA, Conard J, Pabinger I, Ryan K, Bauer KA, Bhavnani M, Abildgaard U, Finazzi G, et al. 1993. Identification of nine novel mutations in type I antithrombin deficiency by heteroduplex screening. *Brit J Haematol 84*:656–661.

Davis RL, Shrimpton AE, Holohan PD, Bradshaw C, Feiglin D, Sonderegger P, Kinter J, Becker LM, Lacbawan F, Krasnewich D, et al. 1999. Familial dementia caused by polymerisation of mutant neuroserpin. *Nature 401*:376–379.

Delarue M, Samama J-P, Mourey L, Moras D. 1990. Crystal structure of bovine antithrombin III. *Acta Crystallogr B46*:550–556.

Elliott PR, Abrahams J-P, Lomas DA. 1998. Wild type α_1-antitrypsin is in the canonical inhibitory conformation. *J Mol Biol 275*:419–425.

Elliott PR, Lomas DA, Carrell RW, Abrahams J-P. 1996. Inhibitory conformation of the reactive loop of α_1-antitrypsin. *Nat Struct Biol 3*:676–681.

Engh R, Löbermann H, Schneider M, Weigand G, Huber R, Laurell C-B. 1989. The S variant of human α_1-antitrypsin, structure and implications for function and metabolism. *Protein Eng 2*:407–415.

Gooptu B, Hazes B, Chang W-SW, Dafforn TR, Carrell RW, Read R, Lomas DA. 2000. New inactive conformation of the serpin α_1-antichymotrypsin indicates two stage insertion of the reactive loop; implications for inhibitory function and conformational disease. *Proc Natl Acad Sci USA 97*:67–72.

Harrop SJ, Jankova L, Coles M, Jardine D, Whittaker JS, Gould AR, Meister A, King GC, Mabbutt BC, Curmi PMG. 1998. The crystal structure of plasminogen activator inhibitor 2 at 2.0 Å resolution: Implications for serpin function. *Structure 7*:43–45.

Jeunemaitre X, Soubrier F, Kotelevtsev YV, Lifton RP, Williams CS, Charru A, Hunt SC, Hopkins PN, Williams RR, Lalouel J-M, et al. 1992. Molecular basis of human hypertension: Role of angiotensinogen. *Cell 71*:169–180.

Jin L, Abrahams J-P, Skinner R, Petitou M, Pike R, Carrell RW. 1997. The anticoagulant activation of antithrombin by heparin. *Proc Natl Acad Sci USA 94*:14683–14688.

Jones TA, Zou J-Y, Cowan SW, Kjeldgaard M. 1991. Improved methods for building protein models in electron density maps and the location of errors in these models. *Acta Crystallogr A 47*:110–119.

Kleywegt GJ, Brünger AT. 1996. Checking your imagination: Applications of the free *R* value. *Structure 4*:897–904.

Kraulis PJ. 1991. MOLSCRIPT: A program to produce both detailed and schematic plots of protein structures. *J Appl Crystallogr 24*:946–950.

Laskowski RA. 1995. SURFNET: A program for visualizing molecular surfaces, cavities, and intermolecular interactions. *J Mol Graph 13*:323–330.

Lawrence DA. 1997. The serpin-proteinase complex revealed. *Nat Struct Biol 4*(5):339–341.

Lee KN, Park SD, Yu M-H. 1996. Probing the native strain in α_1-antitrypsin. *Nat Struct Biol 3*:497–500.

Leslie AWG. 1992. Recent changes to the MOSFLM package for processing film and image data. *Joint CCP4 and ESF-EACMB Newsletter on Protein Crystallography*. Warrington, UK: Daresbury Laboratory.

Li J, Wang Z, Canagarajah B, Jiang H, Kanost M, Goldsmith EJ. 1999. The structure of active serpin 1K from *Manduca sexta*. *Structure 7*:103–109.

Loebermann H, Tokuoka R, Deisenhofer J, Huber R. 1984. Human α_1-proteinase inhibitor. Crystal structure analysis of two crystal modifications, molecular model, and preliminary analysis of the implications for function. *J Mol Biol 177*:531–556.

Lomas DA, Evans DL, Stone SR, Chang W-SW, Carrell RW. 1993. Effect of the Z mutation on the physical and inhibitory properties of α_1-antitrypsin. *Biochemistry 32*:500–508.

Machin PA, Campell JW, Elder M. 1980. Refinement of protein structures. *Proceedings of the Daresbury Study Weekend*. Warrington, UK: SERC Daresbury Laboratory.

Mast AE, Enghild JJ, Salvesen G. 1992. Conformation of the reactive site loop of α_1-proteinase inhibitor probed by limited proteolysis. *Biochemistry 31*:2720–2728.

Mori Y, Seino S, Takeda K, Flink IL, Murata Y, Bell GI, Refetoff S. 1989. A mutation causing reduced biological activity and stability of thyroxine-binding globulin probably as a result of abnormal glycosylation of the molecule. *Mol Endocrinol 3*:575–579.

Mottonen J, Strand A, Symersky J, Sweet RM, Danley DE, Geoghegan KF, Gerard RD, Goldsmith EJ. 1992. Structural basis of latency in plasminogen activator inhibitor-1. *Nature 355*:270–273.

Mourey L, Samama J-P, Delarue M, Petitou M, Choay J, Moras D. 1993. Crystal structure of cleaved bovine antithrombin III at 3.2 Å resolution. *J Mol Biol 232*:223–241.

Murshudov GN, Vagin AA, Dodson EJ. 1997. Refinement of macromolecular structures by the maximum-likelihood method. *Acta Crystallogr D53*:240–255.

Navaza J. 1994. AMoRe: An automated package for molecular replacement. *Acta Crystallogr A50*:157–163.

Pannu NS, Read RJ. 1996. Improved structure refinement throught maximum likelihood. *Acta Crystallogr A52*:659–668.

Patston PA, Hauert J, Michaud M, Schapira M. 1995. Formation and properties of C1-inhibitor polymers. *FEBS Lett 368*:401–404.

Potempa J, Korzus E, Travis J. 1994. The serpin superfamily of proteinase inhibitors: Structure, function, and regulation. *J Biol Chem 269*:15957–15960.

Read RJ. 1986. Improved Fourier coefficients for maps using phases from partial structures with errors. *Acta Crystallogr A42*:140–149.

Rice LM, Brünger AT. 1994. Torsion angle dynamics: Reduced variable conformational sampling enhances crystallographic structure refinement. *Proteins Struct Funct Genet 19*:277–290.

Ryu S-E, Choi H-J, Kwon K-S, Lee KN, Yu M-H. 1996. The native strains in the hydrophobic core and flexible reactive loop of a serine protease inhibitor: Crystal structure of an uncleaved α_1-antitrypsin at 2.7 Å. *Structure 4*:1181–1192.

Schreuder HA, de Boer B, Dijkema R, Mulders J, Theunissen HJM, Grootenhuis PDJ, Hol WGJ. 1994. The intact and cleaved human antithrombin III complex as a model for serpin-proteinase interactions. *Nat Struct Biol 1*: 48–54.

Sharp AM, Stein PE, Pannu NS, Carrell RW, Berkenpas MB, Ginsburg D, Lawrence DA, Read RJ. 1999. The active conformation of plasminogen activator inhibitor 1, a target for drugs to control fibrinolysis and cell adhesion. *Structure 7*:111–118.

Skinner R, Abrahams J-P, Whisstock JC, Lesk AM, Carrell RW, Wardell MR. 1997. The 2.6 Å structure of antithrombin indicates a conformational change at the heparin binding site. *J Mol Biol 266*:601–609.

Stein PE, Carrell RW. 1995. What do dysfunctional serpins tell us about molecular mobility and disease? *Nat Struct Biol 2*:96–113.

Stein PE, Leslie AGW, Finch JT, Turnell WG, McLaughlin PJ, Carrell RW. 1990. Crystal structure of ovalbumin as a model for the reactive center of serpins. *Nature 347*:99–102.

Sui G-C, Wiman B. 1998. Functional effects of single amino acid substitutions in the region of Phe113 to Asp138 in the plasminogen activator inhibitor 1 molecule. *Biochem J 331*:409–415.

Wei A, Rubin H, Cooperman BS, Christianson DW. 1994. Crystal structure of an uncleaved serpin reveals the conformation of an inhibitory reactive loop. *Nat Struct Biol 1*:251–258.

Whistock J. 1996. Analysis of conformational change using structural comparisons and modelling studies of serpins. Cambridge: University of Cambridge.